Inhibition of heat shock protein 90 decreases ACTH production and cell proliferation in AtT-20 cells

(AtT-20 細胞における Hsp90 阻害による ACTH 産生及び細胞増殖の抑制作用)

申請者　弘前大学大学院医学研究科

病態制御科学領域内分泌代謝内科学教育研究分野

氏名　杉山　綾

指導教授　大門　眞

Abstract

Purpose

Cushing's disease is primarily caused by adrenocorticotropic hormone (ACTH)-producing pituitary adenomas. If excision of the tumor from the pituitary, which is the primary treatment for Cushing's disease, is unsuccessful, further medical therapy is needed to treat the resultant hypercortisolism. Some of the drugs used to treat this condition have shown potential therapeutic benefits, but a more effective treatment should be explored for the treatment of Cushing's disease. In the present study, we determined the effect of heat shock protein 90 (Hsp90) inhibitors on ACTH production and cell proliferation of AtT-20 corticotroph tumor cells.

Methods

AtT-20 pituitary corticotroph tumor cells were cultured. The expression levels of mouse proopiomelanocortin (POMC) and pituitary tumor transforming gene 1 (PTTG1) mRNA were evaluated using quantitative real-time PCR. Cellular DNA content was analyzed with fluorescence-activated cell sorting (FACS) analysis. The protein levels were determined by Western blot analysis.

Results

Both 17-allylamino-17-demethoxygeldanamycin (17-AAG) and CCT018159 decreased POMC mRNA levels in AtT-20 cells and ACTH levels in the culture medium of these cells, suggesting that both drugs suppress ACTH synthesis and secretion in corticotroph tumor cells. Both drugs also decreased cell proliferation and induced apoptosis. FACS analyses revealed that both agents increased the percentage of AtT-20 cells in the G2/M phase. These drugs decreased cell proliferation, presumably due to the induction of cell death and arrest of the cell cycle in AtT-20 cells. Tumor weight in mice xenografted with AtT-20 cells and treated with CCT018159 was lower than in AtT-20-xenografted control mice. CCT018159 also decreased plasma ACTH

levels, and POMC and PTTG1 mRNA levels in the tumor cells.

Conclusions

CCT018159 inhibits ACTH production and corticotroph tumor cell proliferation *in vitro* and *in vivo*.

Introduction

Cushing's disease is primarily caused by adrenocorticotropic hormone (ACTH)-producing pituitary adenomas [1, 2]. The normal cortisol feedback mechanism of the hypothalamic-pituitary-adrenal axis is disturbed, resulting in hypercortisolism that causes metabolic derangements such as diabetes mellitus, hypertension, atherosclerosis, and immune dysfunction [3]. Excision of the tumor from the pituitary is the primary treatment for Cushing's disease; however, if excision is unsuccessful, further therapy is needed to treat the resultant hypercortisolism [4, 5]. These therapies include repeat pituitary surgery, radiotherapy, or medical therapy. Various somatostatin receptor agonists have demonstrated inhibitory effects on tumor cell proliferation in pituitary tumors, including somatotroph and thyrotroph tumors. In some patients with Cushing's disease, SOM230 has shown promising effects by decreasing the levels of plasma ACTH and urinary free cortisol [6, 7]. Novel somatostatin-dopamine chimeric molecules or retinoic acid also appear to be a promising approach [8, 9]. Retinoic acid and curcumin may be developed as a novel therapeutic agents [10, 11]. However, a more effective medical therapy should be explored for the treatment of Cushing's disease.

Tumor growth is at least partially regulated by cell proliferation, cell cycle progression, and apoptosis. Pituitary tumor transforming gene 1 (PTTG1) is an oncogene that was first cloned from a rat pituitary tumor [12]. PTTG1 is overexpressed in many types of cancer from various origins [13]. PTTG1 is a hallmark of pituitary tumors [14, 15], and it facilitates cell cycle progression, increases pituitary cell proliferation, and promotes murine pituitary development [16].

Heat shock protein 90 (Hsp90) is an essential molecular chaperone involved in the folding and stabilization of client proteins that regulate the survival of cancer cells. Hsp90 inhibitors are promising targeted cancer therapeutic drugs that are now in clinical

trial. Geldanamycin, an ansamycin benzoquinone antibiotic and Hsp90 inhibitor, has shown antitumor effects in various tumor cells. Hsp90 inhibitors reportedly repress PTTG1 expression in carcinoma cells [17, 18], and they are expected to act on pituitary tumor cells. 17-Allylamino-17-demethoxygeldanamycin (17-AAG) (IC_{50} = 7.2 μM) is a less toxic and potent synthetic derivative of geldanamycin. CCT018159 (IC_{50} = 3.2 μM) is a structurally dissimilar Hsp90 inhibitor; it is a cell-permeable pyrazole resorcinol compound that inhibits the ATPase activity of Hsp90. CCT018159 exhibits similar cellular properties to 17-AAG with potential advantages, such as aqueous solubility and independence from polymorphic enzymes [19]. Further, the effects of hypercortisolism may be reduced using Hsp90 inhibitors, because glucocorticoid receptors require Hsp90 for ligand binding.

In the present study, we examined the effects of Hsp90 inhibitors on ACTH production and cellular proliferation in AtT-20 corticotroph tumor cells. To elucidate further the possible effects of the Hsp90 inhibitors *in vivo*, we then examined, for the first time, the effects of CCT018159 on various parameters, including body weight, tumor weight, tumor PTTG1 and proopiomelanocortin (POMC) mRNA levels, and plasma ACTH and corticosterone levels, in AtT-20-xenografted mice.

Materials and Methods

Hsp90 inhibitors

17-AAG and CCT018159 were purchased from Wako Pure Chemical Industries (Osaka, Japan) and Tocris Bioscience (Ellisville, MO), respectively. Each inhibitor was dissolved in dimethyl sulfoxide (DMSO), diluted by cell culture medium, and used as concentrations between 100 nM and 10 μM.

Cell culture

AtT-20 pituitary corticotroph tumor cells were cultured in a T_{75} culture flask with Dulbecco's modified Eagle's medium (DMEM) supplemented with 10% fetal bovine serum (FBS), 100 μg/mL streptomycin, and 100 U/mL penicillin at 37°C in a humidified atmosphere of 5% CO_2 and 95% air. The cells were plated in 6-well plates at 1.5×10^5 cells/well for 2 days before each experiment and the medium was changed every 48 h. On day 3, to remove the effect of factors contained in FBS, the cells were washed and then starved overnight with DMEM supplemented with 0.2% bovine serum albumin prior to each experiment. At the end of each experiment, total cellular RNA or protein was collected and stored at -80°C until the relevant assay was performed.

Xenograft experiments

All animal studies were approved by the Institute for Animal Experiments, Hirosaki University School of Medicine and the Institutional Review Board of Hirosaki University School of Medicine. Male KSN/Slc nude mice at 8 weeks of age (approximate 22–24 g) were purchased from Japan SLC, Inc. (Shizuoka, Japan) and maintained in pathogen-free conditions. The mice were injected subcutaneously with AtT-20 cells (5.0×10^6 cells/mouse) in vehicle (200 μL) and divided randomly into 2 groups: control (vehicle only, n = 8) and CCT018159 (4 mg/mouse per day, n = 7). CCT018159,

dissolved in vehicle (DMSO and 0.9% saline), was administered subcutaneously once a day for 14 days from 2 weeks after AtT-20 cell injection. We selected 4 mg CCT018159/mouse per day because this dose was used previously to show its pharmacokinetic and metabolic properties in rodents *in vivo* [20]. At the end of the experiment, the mice were killed and tumor weights were measured after their careful resection. All mice were killed from 02:00 to 03:00 PM. The tumors were used for a quantitative real-time RT-PCR assay. Trunk blood was also collected for blood glucose and corticosterone assays. Blood glucose levels were measured using Nipro StatStrip XP (Nipro, Osaka, Japan) at the time of the experiment.

RNA extraction

The cells were incubated with medium alone (control) or medium containing 17-AAG or CCT018159 for the indicated times. To examine the dose-dependent effects of 17-AAG or CCT018159, the cells were incubated for the indicated times with medium alone (control) or medium containing increasing concentrations of 17-AAG or CCT018159 (100 nM–10 μM). At the end of each experiment, total cellular RNA was extracted using RNeasy Mini Kit (QIAGEN, Hilden, Germany) according to the manufacturer's protocol. Complementary DNA (cDNA) was synthesized from total RNA (0.5 μg) using random hexamers as primers with the SuperScript First-Strand Synthesis System for Reverse Transcriptase-Polymerase Chain Reaction (RT-PCR) (Invitrogen Corp., Carlsbad, CA) according to the manufacturer's instructions.

Quantitative real-time RT-PCR

Total cellular RNA extraction and cDNA synthesis were performed as described previously [21, 22]. The resulting cDNA was then subjected to real-time PCR as follows. The expression levels of mouse POMC (NM_008895.3) and PTTG1 (NM_001131054.1)

mRNA were evaluated using quantitative real-time PCR with specific sets of primers and probes (Assays-on-Demand Gene Expression Products; Applied Biosystems, Foster City, CA). β2-Microglobulin (B2MG) was used as a reference gene to standardize expression levels because B2MG mRNA levels did not change during any treatments in this study. Each reaction consisted of 1× TaqMan Universal PCR Master Mix (Applied Biosystems), 1× Assays-on-Demand Gene Expression Products (Mm00435874_m1 for mouse POMC, Mm00479224_m1 for mouse PTTG1, and Mm00437762_m1 for mouse B2MG), and 500 ng cDNA in a total volume of 25 µL with the following parameters on an ABI PRISM 7000 Sequence Detection System (Applied Biosystems): 95°C for 10 min and then 40 cycles at 95°C for 15 s and 60°C for 1 min.

The above assays involved specific sets of primers and a TaqMan probe spanning the exon–exon junction and should not, therefore, have been affected by DNA contamination. Data were collected and recorded with ABI PRISM 7000 SDS software (Applied Biosystems) and expressed as a function of the threshold cycle (C_T). The amplification efficacies of each gene of interest and the reference gene amplimers were found to be identical when analyzed with diluted samples.

Relative quantitative gene expression was calculated by the $2^{-\Delta\Delta C_T}$ method. In brief, for each sample assayed, the C_T for the reactions amplifying the gene of interest and a reference gene were determined. The C_T for the gene of interest of each sample was corrected by subtracting the C_T for the housekeeping gene (ΔC_T). Untreated controls were chosen as reference samples, and the ΔC_T for all experimental samples was reduced by the average ΔC_T for the control samples ($\Delta\Delta C_T$). Finally, the abundance of the experimental mRNA relative to that of the control mRNA was calculated with use of the formula $2^{-\Delta\Delta C_T}$.

Western blot analysis

Western blot analysis was performed to examine the protein levels of phosphorylated cyclic adenosine monophosphate response element-binding protein (pCREB)/CREB, phosphorylated extracellular signal-related kinases (pERK)/ERK, and phosphorylated Akt (pAkt)/Akt. β-actin was used as a housekeeping protein. The cells were washed twice with phosphate-buffered saline (PBS) and lysed with Laemmli sample buffer. Cell debris was pelleted by centrifugation and the supernatant was recovered. The samples (6 μg/each sample) were boiled and subjected to electrophoresis on a 4–20% gradient polyacrylamide gel, and the proteins were transferred to a polyvinylidene fluoride membrane (Daiichi Kagaku, Tokyo, Japan). After blocking with Detector Block® buffer (Kirkegaard & Perry Laboratories, Gaithersburg, MD), the membrane was incubated for 1 h with each antibody (anti-pCREB [1:500 dilution]/CREB [1:500 dilution], anti-pERK [1:500 dilution]/ERK [1:500 dilution], and anti-pAkt [1:500 dilution]/Akt [1:2000 dilution] antibodies, Cell Signaling Technology, Beverly, MA; and anti-β-actin [1:1000 dilution] antibody, ab8227 Abcam, Cambridge, MA), washed with PBS containing 0.05% Tween 20, and incubated with horseradish peroxidase-labeled anti-rabbit immunoglobulin G ([1:20000 dilution], Daiichi Kagaku). The chemiluminescent substrate SuperSignal West Pico (Pierce Chemical Co., Rockford, IL) was used for detection and the membrane was exposed to BioMax film (Eastman Kodak Co., Rochester, NY).

ACTH assay

The cells were incubated at 37°C for 24 h with the indicated concentrations of 17-AAG or CCT018159. The media were then aspirated and the ACTH levels in the supernatants were measured using an ACTH enzyme-linked immunosorbent assay (ELISA) kit (MD Bioproducts, Zurich, Switzerland). The blood samples were centrifuged

and the ELISA kit was used to measure plasma ACTH levels. All samples from each experiment were determined in the same assay. The intra- and inter-assay coefficients of variation (CV) were 6.7% at 42.2 pg/mL and 7.1% at 42.3 pg/mL, respectively. Cross-reactivities with ACTH (1–24), ACTH (18–39), and α-melanocyte-stimulating hormone were -3.4%, -2.4%, and -1.7%, respectively.

Cell proliferation assay

The cells were incubated at 37°C for 48 h with the indicated concentrations of 17-AAG or CCT018159. Viable cells were measured using a Cell Counting Kit-8 (Dojin, Kumamoto, Japan). All samples from each experiment were determined in the same assay.

Cell death detection assay

The cells were incubated at 37°C for 24 h with the indicated concentrations of 17-AAG or CCT018159. DNA fragmentation was measured using a Cell Death Detection ELISA Kit (Roche, Penzberg, Germany), and each enrichment factor was calculated according to the manufacturer's instructions.

Cell cycle analysis

AtT-20 cells were incubated for 24 h with medium alone (control) or medium containing 10 μM 17-AAG or CCT018159. The cells were collected by trypsinization, pelleted by centrifugation, and suspended in Triton X-100. The cells were treated at 37°C for 30 min with 0.5% RNase A and stained with propidium iodine (50 μg/mL). Cellular DNA content was analyzed with fluorescence-activated cell sorting (FACS) analysis and the cell cycle profiles were determined with BD FACSDiva^{TM} software (Becton Dickinson, Franklin Lakes, NJ).

Corticosterone assay

The blood samples were centrifuged and a rodent corticosterone ELISA kit (Endocrine Technologies, Newark, CA) was used to measure plasma corticosterone levels. All samples from each experiment were determined in the same assay.

Statistical analysis

Each *in vitro* experiment was performed at least 3 times. Samples were provided in triplicate for each group of experiments. Each value is expressed as the mean ± standard error of the mean. For the *in vitro* studies, statistical analysis was performed with analysis of variance (ANOVA), followed by Fisher's protected least-significant difference post hoc test. For the *in vivo* studies, statistical analysis was performed using an unpaired Student's *t*-test. The level of statistical significance was set at $P < 0.05$.

Results

Effects of 17-AAG and CCT018159 on POMC mRNA levels

AtT-20 cells were incubated with 17-AAG or CCT018159 to determine their effects on the time- and dose-dependent changes of POMC mRNA levels. A time course study showed that 10 µM 17-AAG significantly decreased POMC mRNA levels (ANOVA; $P < 0.01$, Fig. 1A), with POMC mRNA levels falling to 43% of the control value within 24 h of the addition of 10 µM 17-AAG (Fig. 1A). POMC mRNA levels decreased in a dose-dependent manner (ANOVA; $P < 0.0005$), with significant effects observed from 1 to 10 µM (Fig. 1A).

A time course study showed that 10 µM CCT018159 significantly decreased POMC mRNA levels (ANOVA; $P < 0.05$, Fig. 1B), with POMC mRNA levels falling to 72% of the control value within 6 h of the addition of 10 µM CCT018159 (Fig. 1B). POMC mRNA levels decreased in a dose-dependent manner (ANOVA; $P < 0.01$), with significant effects observed at 10 µM (Fig. 1B).

Effects of 17-AAG and CCT018159 on ACTH levels

ACTH levels in the medium also decreased in a dose-dependent manner (ANOVA; $P < 0.005$ [17-AAG] or $P < 0.05$ [CCT018159]), with significant effects observed from 1 to 10 µM 17-AAG (Fig. 2A) or at 10 µM CCT018159 (Fig. 2B).

Effects of 17-AAG and CCT018159 on PTTG1 mRNA levels

A time course study showed that 10 µM 17-AAG potently decreased PTTG1 mRNA levels (ANOVA; $P < 0.005$, Fig. 3A), with PTTG1 mRNA levels falling to 23% of the control value within 24 h of the addition of 10 µM 17-AAG (Fig. 3A). PTTG1 mRNA levels decreased in a dose-dependent manner (ANOVA; $P < 0.005$), with significant effects observed at 10 µM (Fig. 3A).

A time course study showed that 10 µM CCT018159 significantly decreased PTTG1 mRNA levels (ANOVA; $P < 0.005$, Fig. 3B), with PTTG1 mRNA levels falling to 57% of the control value within 6 h of the addition of 10 µM CCT018159 (Fig. 3B). PTTG1 mRNA levels decreased in a dose-dependent manner (ANOVA; $P < 0.05$), with significant effects observed at 10 µM (Fig. 3B).

Time-dependent changes in 17-AAG- and CCT018159-induced CREB, ERK, and Akt phosphorylation

AtT-20 cells were incubated with 10 µM 17-AAG or CCT018159 to determine their effects on CREB, ERK, and Akt phosphorylation. A time course study showed that 17-AAG decreased both CREB and ERK phosphorylation from 5 min to 6 h, while it increased Akt phosphorylation from 5 to 30 min in AtT-20 cells (Fig. 4A). CCT018159 also decreased both CREB and ERK phosphorylation from 5 min to 6 h, while it increased Akt phosphorylation from 30 min to 2 h in AtT-20 cells (Fig. 4B).

Effects of 17-AAG and CCT018159 on cell proliferation

AtT-20 cells were incubated with 17-AAG or CCT018159 to determine their effects on the dose-dependent changes in cell proliferation. The study showed that 10 µM 17-AAG (Fig. 5A) or 10 µM CCT018159 (Fig. 5B) significantly decreased cell proliferation (ANOVA; $P < 0.0001$ [17-AAG] or $P < 0.001$ [CCT018159]).

Effects of 17-AAG and CCT018159 on cell death

To examine whether 17-AAG and CCT018159 induced cell death, cytoplasmic histone-associated DNA fragmentation was determined. DNA fragmentation increased in a dose-dependent manner (ANOVA; $P < 0.0001$ [17-AAG] or $P < 0.0001$ [CCT018159]), with significant effects observed from 100 nM to 10 µM 17-AAG (Fig. 6A)

or 10 μM CCT018159 (Fig. 6B).

Effects of 17-AAG and CCT018159 on cell cycle profiles

Cell cycle distribution was assessed using flow cytometry. FACS analyses revealed that the percentage of cells in the S phase was decreased after incubation with 10 μM 17-AAG, and the percentage in the G2/M phase was increased after incubation with 10 μM 17-AAG or 10 μM CCT018159 (Fig. 7).

Effects of CCT018159 on the physiology of AtT-20-xenografted mice

AtT-20-xenografted mice produce high levels of plasma corticosterone levels and have been used as an animal model of ACTH-dependent Cushing's disease (Taguchi *et al*. 2006, Fukuoka *et al*. 2011). AtT-20-xenografted mice were treated with CCT018159 to determine its effects on corticotroph tumor growth and function *in vivo*. In control (vehicle) mice xenografted with AtT-20 cells, body weight decreased during the study period (14 days). The decrease in body weight was significantly smaller following treatment with CCT018159 ($P < 0.01$; Fig. 8A). Tumor weight in mice treated with CCT018159 was significantly lower than in control mice ($P < 0.05$; Fig. 8B). CCT018159 also significantly decreased tumor PTTG1 and POMC mRNA levels compared with control ($P < 0.05$; Fig. 8C and 8D). Finally, CCT01859 significantly decreased plasma ACTH levels compared with control ($P < 0.05$; Fig. 8E). Plasma corticosterone levels were significantly lower following treatment with CCT018159 ($P < 0.01$; Fig. 8F). Blood glucose levels were unaltered in CCT018159-treated mice (Fig. 8G).

Discussion

Recent studies suggested that Hsp90 inhibitors are promising drugs for treating various cancers, including breast cancer, esophageal squamous cell carcinoma, and melanoma [23-25], and are now in clinical trial. In this study, we found that the Hsp90 inhibitors 17-AAG and CCT018159 decreased POMC mRNA levels in AtT-20 cells and the basal levels of ACTH in the culture medium of these cells. These results suggest that these Hsp90 inhibitors suppress the autonomic production, as well as the synthesis and release, of ACTH in corticotroph tumor cells.

Both 17-AAG and CCT018159 decreased cell proliferation in AtT-20 cells. These drugs increased DNA fragmentation in AtT-20 cells, suggesting that they induced cell death in corticotroph tumor cells. 17-AAG induces G1 arrest in prostate cancer cells [26], while it also induces G2/M arrest in lung cancer cells [27]. FACS analyses revealed that these drugs increased the percentage of AtT-20 cells in the G2/M phase, although they provoked a differential action in the S phase. G2 arrest is often associated with DNA damage; therefore, these drugs may attenuate cell cycle progression or cause cell arrest at the G2/M phase, resulting in the inhibition of cell proliferation. Decreases in cell numbers may contribute to decreases in ACTH production. Additionally, in the present study, both 17-AAG and CCT018159 gradually decreased PTTG1 mRNA levels in AtT-20 cells. Hsp90 inhibitors repress PTTG1 mRNA levels in human colon carcinoma cells [17, 18]. PTTG1 facilitates cell cycle progression and increases pituitary cell proliferation [16]. PTTG1 overexpression results in the proliferation of pituitary gonadotroph cells [15]. These findings indicate that PTTG1may be involved in the Hsp90 inhibitor-induced suppression of cell proliferation in AtT-20 cells. Further study in the future is expected at this point.

In the present study, both 17-AAG and CCT018159 decreased CREB and ERK phosphorylation. CREB phosphorylation is increased by corticotropin-releasing factor

(CRF) via the protein kinase A (PKA) pathway in AtT-20 cells [28]. The PKA pathway has an important role in the regulation of POMC gene expression and the desensitization of CRF receptor type 1 by CRF in corticotroph cells [28, 29]. Both 17-AAG and CCT018159 decreased CREB phosphorylation in AtT-20 cells, presumably resulting in the inhibition of ACTH synthesis via the PKA pathway. ERK phosphorylation is also caused by CRF in AtT-20 cells [28]. Inhibition of the CRF-induced phosphorylation of ERK and p38 is involved in the suppression of ACTH production [30]. These decreases of CREB and ERK phosphorylation would be involved in the pathway to suppress ACTH production.

Conversely, both agents increased Akt phosphorylation. The phosphoinositide 3-kinase/Akt pathway is an intracellular signaling pathway that contributes to apoptosis or inhibition of proliferation in pituitary tumor cells [31]. Generally, this pathway is overactive in a variety of cancer cells, and 17-AAG inhibits Akt activation and expression, and shows an antiproliferative action in tumors [32]. In pituitary tumors, including thyrotroph and corticotroph tumor cells, Akt expression levels are upregulated [33, 34]. However, it is unclear what role Hsp90 inhibitor-induced Akt phosphorylation has in pituitary corticotroph tumor cells. Treatment with rapamycin, a mammalian target of rapamycin inhibitor, also reportedly increases Akt phosphorylation due to the abolition of a negative feedback loop that blunts phosphoinositide 3-kinase-mediated support for Akt activation, resulting in a reduction of sensitivity to rapamycin [35]. In this case, the addition of a somatostatin analog to rapamycin decreased Akt phosphorylation, resulting in an improvement of the antiproliferative action of this treatment in AtT-20 cells. Therefore, in addition to an Hsp90 inhibitor, adjuvant treatment with a somatostatin analog may sensitize cells to the antiproliferative effects of Hsp90 inhibitors in AtT-20 cells.

In control mice xenografted with AtT-20 cells, body weight was decreased. The

present results are consistent with those of earlier studies showing that mice with Cushing's syndrome lose weight [36]. CCT018159 exhibits similar cellular properties to 17-AAG with potential advantages, such as aqueous solubility, for an *in vivo* use. Therefore, AtT-20-xenografted mice were treated with CCT018159 to determine its effects on corticotroph tumor growth and function *in vivo*. Tumor weight in mice treated with CCT018159 was lower than in control mice, suggesting that CCT018159 may suppress cell proliferation *in vivo*. In this study, CCT018159 also decreased tumor PTTG1 mRNA levels *in vivo*. Together, these findings indicate that PTTG1 may be partially involved in the CCT018159-induced suppression of cell proliferation in mice xenografted with AtT-20 cells.

Treatment with CCT018159 decreased tumor POMC levels, suggesting that CCT018159 suppresses ACTH synthesis *in vivo*. Cushing's disease is characterized by ACTH-dependent excessive circulating glucocorticoid concentrations. Therefore, plasma ACTH and corticosterone levels have been measured *in vivo* [36, 37]. CCT01859 suppressed plasma ACTH levels directly via the tumor production even *in vivo*. Finally, plasma corticosterone levels were also decreased following treatment with CCT018159. However, the difference between ACTH levels and corticosterone levels was found in this study. Autonomous/dysregulated mild secretion of ACTH may cause excess cortisol production [38]. Otherwise, plasma corticosterone levels may be modulated via other stress factors or conditions in addition to stimulation of ACTH *in vivo*. Thus, this Hsp90 inhibitor should have suppressive effects on ACTH-dependent hypercortisolemia.

Conclusion

The present study demonstrated that 17-AAG and CCT018159 decrease POMC mRNA levels in AtT-20 cells and ACTH levels in the culture medium of these cells.

These drugs decrease cell proliferation, presumably due to the induction of cell death and cell cycle arrest in AtT-20 cells. Tumor weight in mice xenografted with AtT-20 cells and treated with CCT018159 was significantly lower than that in control mice. CCT018159 also significantly decreases plasma ACTH levels, and tumor PTTG1 and POMC mRNA levels. Thus, CCT018159 shows inhibitory effects on ACTH production and corticotroph tumor cell proliferation *in vitro* and *in vivo*.

Conflict of interest

None of the authors have any potential conflicts of interest associated with this research.

Acknowledgments

We thank the Department of Social Medicine, Hirosaki University Graduate School of Medicine, for generously providing us with FACS analysis. This research did not receive any specific grant from any funding agency in the public, commercial or not-for-profit sector.

References

1. Nieman LK, Biller BM, Findling JW, Newell-Price J, Savage MO, Stewart PM, Montori VM (2008) The diagnosis of Cushing's syndrome: an Endocrine Society Clinical Practice Guideline. J Clin Endocrinol Metab 93: 1526-1540

2. Kageyama K, Oki T, Sakihara S, Nigawara T, Terui K, Suda T (2013) Evaluation of the diagnostic criteria for Cushing’s disease in Japan. Endocr J 6: 127-135

3. Biller BM, Grossman AB, Stewart PM, Melmed S, Bertagna X, Bertherat J, Buchfelder M, Colao A, Hermus AR, Hofland LJ, Klibanski A, Lacroix A, Lindsay JR, Newell-Price J, Nieman LK, Petersenn S, Sonino N, Stalla GK, Swearingen B, Vance ML, Wass JA, Boscaro M (2008) Treatment of adrenocorticotropin-dependent Cushing’s syndrome; a consensus statement. J Clin Endocrinol Metab 93: 2454-3462

4. Bertagna X, Guignat L (2013) Approach to the Cushing's disease patient with persistent/recurrent hypercortisolism after pituitary surgery. J Clin Endocrinol Metab 98: 1307-1318

5. Schteingart DE (2009) Drugs in the medical treatment of Cushing's syndrome. Expert Opin Emerg Drugs 14: 661-671

6. Feelders RA, de Bruin C, Pereira AM, Romijn JA, Netea-Maier RT, Hermus AR, Zelissen PM, van Heerebeek R, de Jong FH, van der Lely AJ, de Herder WW, Hofland LJ, Lamberts SW (2010) Pasireotide alone or with cabergoline and ketoconazole in Cushing's disease. N Eng J Med 362: 1846-1848

7. Hofland LJ (2008) Somatostatin and somatostatin receptors in Cushing's disease. Mol Cell Endocrinol 286: 199-205

8. de Bruin C, Feelders RA, Lamberts SW, Hofland LJ (2009) Somatostatin and dopamine receptors as targets for medical treatment of Cushing's Syndrome. Rev Endocr Metab Disord 10: 91-102

9. Ferone D, Gatto F, Arvigo M, Resmini E, Boschetti M, Teti C, Esposito D, Minuto F

(2009) The clinical-molecular interface of somatostatin, dopamine and their receptors in pituitary pathophysiology. J Mol Endocrinol 42: 361-370

10. Páez-Pereda M, Kovalovsky D, Hopfner U, Theodoropoulou M, Pagotto U, Uhl E, Losa M, Stalla J, Grübler Y, Missale C, Arzt E, Stalla GK (2001) Retinoic acid prevents experimental Cushing syndrome. J Clin Invest 108: 1123-1131

11. Bangaru ML, Woodliff J, Raff H, Kansra S (2010) Growth suppression of mouse pituitary corticotroph tumor AtT20 cells by curcumin: a model for treating Cushing's disease. PLoS One 5: e9893

12. Pei L, Melmed S (1997) Isolation and characterization of a pituitary tumor-transforming gene (PTTG). Mol Endocrinol 11: 433-441

13. Vlotides G, Eigler T, Melmed S (2007) Pituitary tumor-transforming gene: physiology and implications for tumorigenesis. Endocr Rev 28: 165-186

14. Zhang X, Horwitz GA, Heaney AP, Nakashima M, Prezant TR, Bronstein MD, Melmed S (1999) Pituitary tumor transforming gene (PTTG) expression in pituitary adenomas. J Clin Endocrinol Metab 84: 761-767

15. Chesnokova V, Zonis S, Zhou C, Ben-Shlomo A, Wawrowsky K, Toledano Y, Tong Y, Kovacs K, Scheithauer B, Melmed S (2011) Lineage-specific restraint of pituitary gonadotroph cell adenoma growth. PLoS One 6: e17924

16. Chesnokova V, Zonis S, Wawrowsky K, Tani Y, Ben-Shlomo A, Ljubimov V, Mamelak A, Bannykh S, Melmed S (2012) Clusterin and FOXL2 act concordantly to regulate pituitary gonadotroph adenoma growth. Mol Endocrinol 26: 2092-2103

17. Hernández A, López-Lluch G, Bernal JA, Navas P, Pintor-Toro JA (2008) Dicoumarol down-regulates human PTTG1/Securin mRNA expression through inhibition of Hsp90. Mol Cancer Ther 7: 474-482

18. Hernández A, López-Lluch G, Navas P, Pintor-Toro JA (2009) HDAC and Hsp90 inhibitors down-regulate PTTG1/securin but do not induce aneuploidy. Genes

Chromosomes Cancer 48: 194-201

19. Sharp SY, Boxall K, Rowlands M, Prodromou C, Roe SM, Maloney A, Powers M, Clarke PA, Box G, Sanderson S, Patterson L, Matthews TP, Cheung KM, Ball K, Hayes A, Raynaud F, Marais R, Pearl L, Eccles S, Aherne W, McDonald E, Workman P (2007) In vitro biological characterization of a novel, synthetic diaryl pyrazole resorcinol class of heat shock protein 90 inhibitors. Cancer Res 67: 2206-2216

20. Smith NF, Hayes A, James K, Nutley BP, McDonald E, Dymock B, Drysdale MJ, Raynaud FI, Workman P (2006) Preclinical pharmacokinetics and metabolism of a novel diaryl pyrazole resorcinol series of heat shock protein 90 inhibitors. Mol Cancer Ther 5: 1628-1637

21. Kageyama K, Hanada K, Suda T (2009) Differential regulation of urocortins1-3 mRNA in human umbilical vein endothelial cells. Regul Pept 155: 131-138

22. Kageyama K, Hanada K, Suda T (2010) Differential regulation and roles of urocortins in human adrenal H295R cells. Regul Pept 162: 18-25

23. Born EJ, Hartman SV, Holstein SA (2013) Targeting HSP90 and monoclonal protein trafficking modulates the unfolded protein response, chaperone regulation and apoptosis in myeloma cells. Blood Cancer J 3: e167

24. Ui T, Morishima K, Saito S, Sakuma Y, Fujii H, Hosoya Y, Ishikawa S, Aburatani H, Fukayama M, Niki T, Yasuda Y (2014) The HSP90 inhibitor 17-N-allylamino-17-demethoxy geldanamycin (17-AAG) synergizes with cisplatin and induces apoptosis in cisplatin-resistant esophageal squamous cell carcinoma cell lines via the Akt/XIAP pathway. Oncol Rep 31: 619-624

25. Zagouri F, Sergentanis TN, Chrysikos D, Papadimitriou CA, Dimopoulos MA, Psaltopoulou T (2013) Hsp90 inhibitors in breast cancer: a systematic review. Breast 22: 569-578

26. Solit DB, Zheng FF, Drobnjak M, Münster PN, Higgins B, Verbel D, Heller G, Tong

W, Cordon-Cardo C, Agus DB, Scher HI, Rosen N (2002) 17-Allylamino-17-demethoxygeldanamycin induces the degradation of androgen receptor and HER-2/neu and inhibits the growth of prostate cancer xenografts. Clin Cancer Res 8: 986-993

27. Senju M, Sueoka N, Sato A, Iwanaga K, Sakao Y, Tominaga M, Irie K, Hayashi S, Sueoka E (2006) Hsp90 inhibitors cause G2/M arrest associated with the reduction of Cdc25C and Cdc2 in lung cancer cell lines. J Cancer Res Clin Oncol 132: 150-158

28. Kageyama K, Hanada K, Moriyama T, Imaizumi T, Satoh K, Suda T (2007) Differential regulation of CREB and ERK phosphorylation through corticotropin-releasing factor receptors type 1 and 2 in AtT-20 and A7r5 cells. Mol Cell Endocrinol 263: 90-102

29. Kageyama K, Hanada K, Moriyama T, Nigawara T, Sakihara S, Suda T (2006) G Protein-coupled receptor kinase 2 involvement in desensitization of corticotropin-releasing factor (CRF) receptor type 1 by CRF in murine corticotrophs. Endocrinology 147: 441-450

30. Tsukamoto N, Otsuka F, Miyoshi T, Yamanaka R, Inagaki K, Yamashita M, Otani H, Takeda M, Suzuki J, Ogura T, Iwasaki Y, Makino H (2010) Effects of bone morphogenetic protein (BMP) on adrenocorticotropin production by pituitary corticotrope cells: involvement of up-regulation of BMP receptor signaling by somatostatin analogs. Endocrinology 151: 1129-1141

31. Theodoropoulou M, Zhang J, Laupheimer S, Paez-Pereda M, Erneux C, Florio T, Pagotto U, Stalla GK (2006) Octreotide, a somatostatin analogue, mediates its antiproliferative action in pituitary tumor cells by altering phosphatidylinositol 3-kinase signaling and inducing Zac1 expression. Cancer Res 66: 1576-1582

32. Solit DB, Basso AD, Olshen AB, Scher HI, Rosen N (2003) Inhibition of heat shock protein 90 function down-regulates Akt kinase and sensitizes tumors to Taxol. Cancer

Res 63: 2139-2144

33. Muşat M, Vax VV, Borboli N, Gueorguiev M, Bonner S, Korbonits M, Grossman AB (2004) Cell cycle dysregulation in pituitary oncogenesis. Front Horm Res 32: 34-62

34. Lu C, Willingham MC, Furuya F, Cheng SY (2008) Activation of phosphatidylinositol 3-kinase signaling promotes aberrant pituitary growth in a mouse model of thyroid-stimulating hormone-secreting pituitary tumors. Endocrinology 149: 3339-3345

35. Cerovac V, Monteserin-Garcia J, Rubinfeld H, Buchfelder M, Losa M, Florio T, Paez-Pereda M, Stalla GK, Theodoropoulou M (2010) The somatostatin analogue octreotide confers sensitivity to rapamycin treatment on pituitary tumor cells. Cancer Res 70: 666-674

36. Taguchi T, Takao T, Iwasaki Y, Nishiyama M, Asaba K, Hashimoto K. (2006) Suppressive effects of dehydroepiandrosterone and the nuclear factor-kappaB inhibitor parthenolide on corticotroph tumor cell growth and function in vitro and in vivo. J Endocrinol 188: 321-331

37. Fukuoka H, Cooper O, Ben-Shlomo A, Mamelak A, Ren SG, Bruyette D, Melmed S (2011) EGFR as a therapeutic target for human, canine, and mouse ACTH-secreting pituitary adenomas. J Clin Invest 121: 4712-4721

38. Kageyama K, Oki Y, Nigawara T, Suda T, Daimon M (2014) Pathophysiology and treatment of subclinical Cushing’s disease and pituitary silent corticotroph adenomas. Endocr J, in press

Figure Legends

Fig. 1. Effects of 17-AAG and CCT018159 on POMC mRNA levels in AtT-20 cells. The cells were treated in triplicate, with the average of 3 independent experiments shown (an average in triplicate was considered n = 1, n = 3). Statistical analysis was performed using one-way ANOVA, followed by Fisher's protected least-significant difference post hoc test. *P < 0.05 (compared with control [C]). **(A)** Time-dependent effects of 17-AAG on POMC mRNA levels (left panel): the cells were incubated with medium containing 10 µM 17-AAG. Dose-dependent effects of 17-AAG on POMC mRNA levels (right panel): the cells were incubated for 24 h with medium containing between 100 nM and 10 µM 17-AAG. **(B)** Time-dependent effects of CCT018159 on POMC mRNA levels (left panel): the cells were incubated with medium containing 10 µM CCT018159 (CCT). Dose-dependent effects of CCT018159 on POMC mRNA levels (right panel): the cells were incubated for 6 h with medium containing between 100 nM and 10 µM CCT018159 (CCT).

Fig. 2. Effects of 17-AAG and CCT018159 on ACTH levels in AtT-20 cells.
The cells were treated in triplicate, with the average of 3 independent experiments shown (an average in triplicate was considered n = 1, n = 3). Statistical analysis was performed using one-way ANOVA, followed by Fisher's protected least-significant difference post hoc test. *P < 0.05 (compared with control [C]). The cells were incubated for 24 h with medium containing between 100 nM and 10 µM 17-AAG or CCT018159 (CCT).

Fig. 3. Effects of 17-AAG and CCT018159 on PTTG1 mRNA levels in AtT-20 cells.
Effects of 17-AAG and CCT018159 on PTTG1 mRNA levels in AtT-20 cells. The cells were treated in triplicate, with the average of 3 independent experiments shown (an

average in triplicate was considered n = 1, n = 3). Statistical analysis was performed using one-way ANOVA, followed by Fisher's protected least-significant difference post hoc test. *P < 0.05 (compared with control [C]). **(A)** Time-dependent effects of 17-AAG on PTTG1 mRNA levels (left panel): the cells were incubated with medium containing 10 μM 17-AAG. Dose-dependent effects of 17-AAG on PTTG1 mRNA levels (right panel): the cells were incubated for 24 h with medium containing between 100 nM and 10 μM 17-AAG. **(B)** Time-dependent effects of CCT018159 on PTTG1 mRNA levels (left panel): the cells were incubated with medium containing 10 μM CCT018159 (CCT). Dose-dependent effects of CCT018159 on PTTG1 mRNA levels (right panel): the cells were incubated for 6 h with medium containing between 100 nM and 10 μM CCT018159 (CCT).

Fig. 4. Time-dependent changes in 17-AAG and CCT018159-induced CREB, ERK, and Akt phosphorylation in AtT-20 cells. The cells were incubated with medium containing 10 μM 17-AAG or CCT018159 (CCT) for the durations shown. Western blot analysis was performed to examine the protein levels of phosphorylated (p) CREB/CREB, pERK/ERK, and pAkt/Akt. Independent experiments were repeated in triplicate and a representative blot is shown.

Fig. 5. Effects of 17-AAG and CCT018159 on cell proliferation in AtT-20 cells. The cells were treated in triplicate, with the average of 3 independent experiments shown (an average in triplicate was considered n = 1, n = 3). Statistical analysis was performed using one-way ANOVA, followed by Fisher's protected least-significant difference post hoc test. *P < 0.05 (compared with control [C]). The cells were incubated for 48 h with medium containing between 100 nM and 10 μM 17-AAG **(A)** or CCT018159 (CCT) **(B)**. Viable cells were measured using a Cell Counting Kit-8.

Fig. 6. Effects of 17-AAG and CCT018159 on cell death in AtT-20 cells. The cells were treated in triplicate, with the average of 3 independent experiments shown (an average in triplicate was considered n = 1, n = 3). Statistical analysis was performed using one-way ANOVA, followed by Fisher's protected least-significant difference post hoc test. *$P < 0.05$ (compared with control [C]). The cells were incubated for 24 h with medium containing between 100 nM and 10 μM 17-AAG **(A)** or CCT018159 (CCT) **(B)**. DNA fragmentation was measured using a Cell Death Detection ELISA Kit.

Fig. 7. Effects of 17-AAG and CCT018159 on cell cycle profiles in AtT-20 cells. Control cells were treated with medium and vehicle. A representative blot is shown in the upper panels. The cells were treated in duplicate, with the average of 3 independent experiments shown in the lower panels (an average in triplicate was considered n = 1, n = 3). Statistical analysis was performed using one-way ANOVA, followed by Fisher's protected least-significant difference post hoc test. *$P < 0.05$ (compared with control [C]). The cells were incubated for 24 h with 10 μM 17-AAG, CCT018159 (CCT), or vehicle containing DMSO. Cellular DNA content was analyzed with FACS analysis and the cell cycle profiles were determined with BD FACSDiva™ software.

Fig. 8. Effects of CCT018159 on the physiology of AtT-20-xenografted mice. N = 8 in AtT-20-xenografted control mice treated with vehicle (C); n = 7 in AtT-20-xenografted mice treated with CCT018159 (CCT). Statistical analysis was performed using an unpaired Student's *t*-test. *$P < 0.05$ (compared with control [C]). **(A)** Changes in body weight. Body weight in each mouse was determined at the end of the experiment (day 14) and compared with that at day 1. **(B)** Changes in tumor weight. Subcutaneous tumors were resected and weighed at the end of the experiment. **(C)** Changes in

PTTG1 mRNA levels in tumors. Total cellular RNA was extracted from the grafted tumor cells and the expression levels of PTTG1 mRNA were determined by real-time RT-PCR. **(D)** Changes in POMC mRNA levels in tumors. Total cellular RNA was extracted from the grafted tumor cells and the expression levels of POMC mRNA were determined by real-time RT-PCR. **(E)** Changes in plasma ACTH levels. Blood was collected at the end of the experiment and the plasma was used in the assay. **(F)** Changes in plasma corticosterone levels. Blood was collected at the end of the experiment and the plasma was used in the assay. **(G)** Changes in blood glucose levels. Blood was collected at the end of the experiment and glucose levels were measured.

Fig.1.

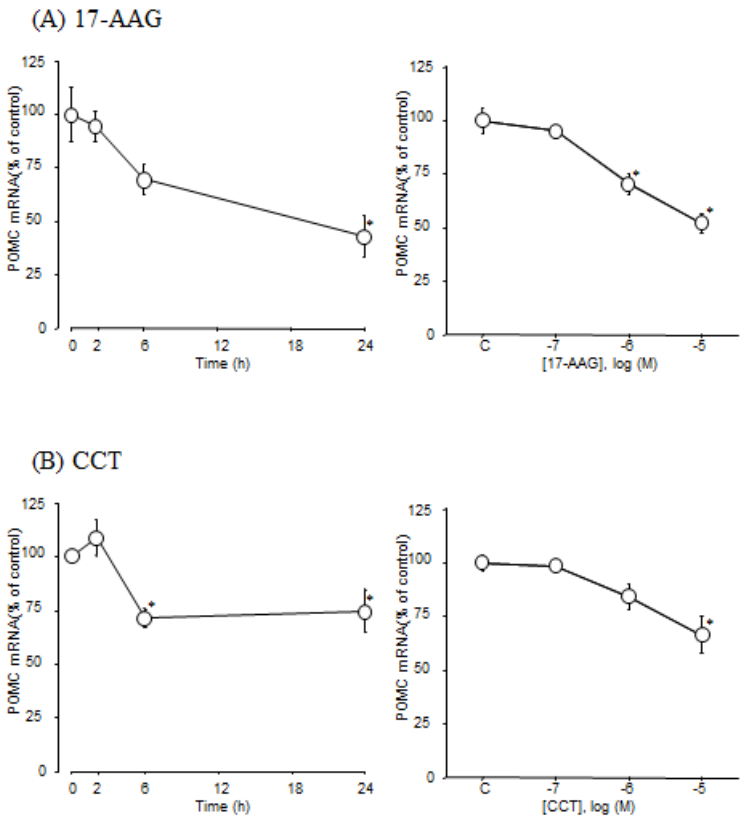
(A) 17-AAG
POMC mRNA(% of control)
125
100
75
50
25
0
0 2 6 12 18 24
Time (h)
C -7 -6 -5
[17-AAG], log (M)
(B) CCT
[CCT], log (M)

Fig.2.

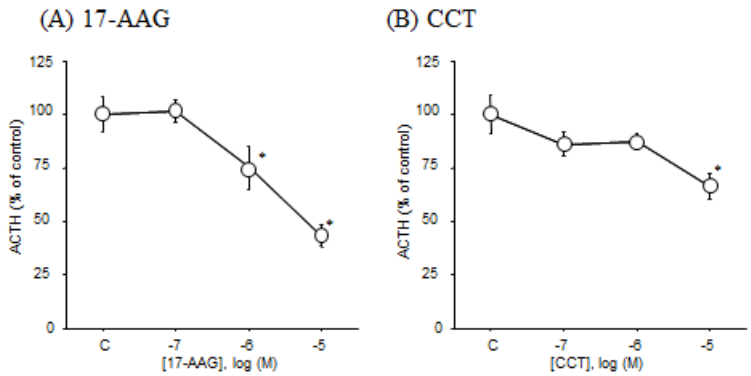
(A) 17-AAG
(B) CCT
ACTH (% of control)
125
100
75
50
25
0
C -7 -6 -5
[17-AAG], log (M)
[CCT], log (M)

Fig.3.

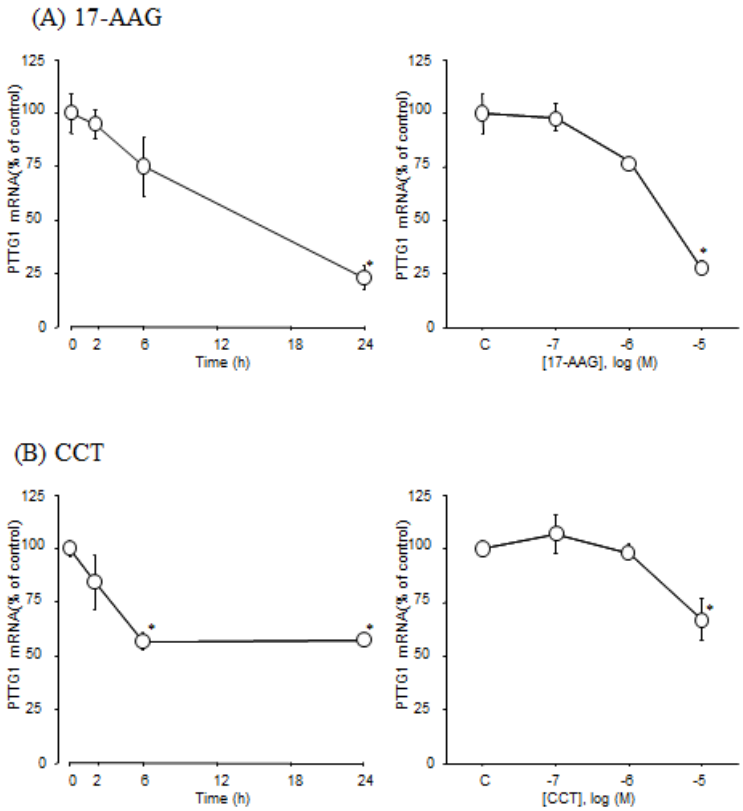
(A) 17-AAG
PTTG1 mRNA(% of control)
125
100
75
50
25
0
0 2 6 12 18 24
Time (h)
C -7 -6 -5
[17-AAG], log (M)
(B) CCT
[CCT], log (M)

Fig.4.

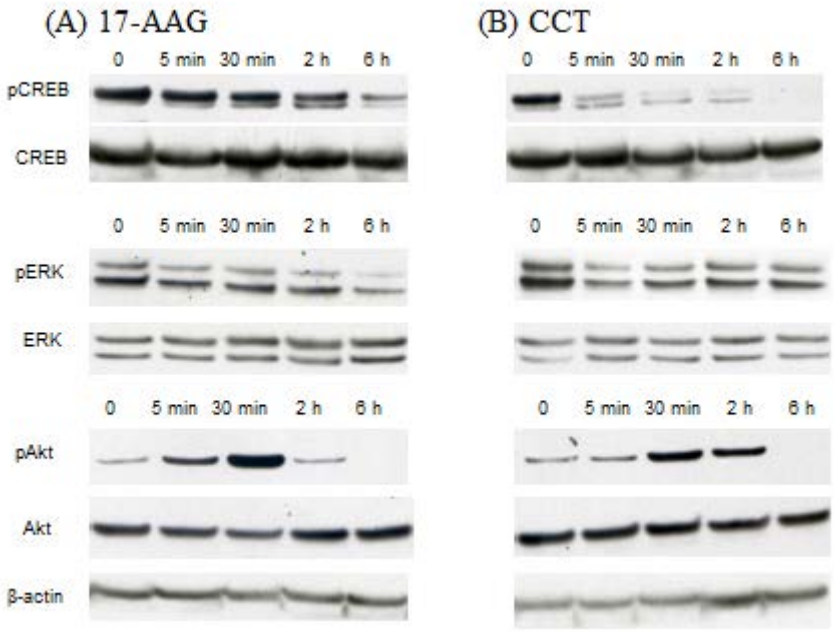
(A) 17-AAG
(B) CCT
0 5 min 30 min 2 h 6 h
pCREB
CREB
pERK
ERK
pAkt
Akt
β-actin

Fig.5.

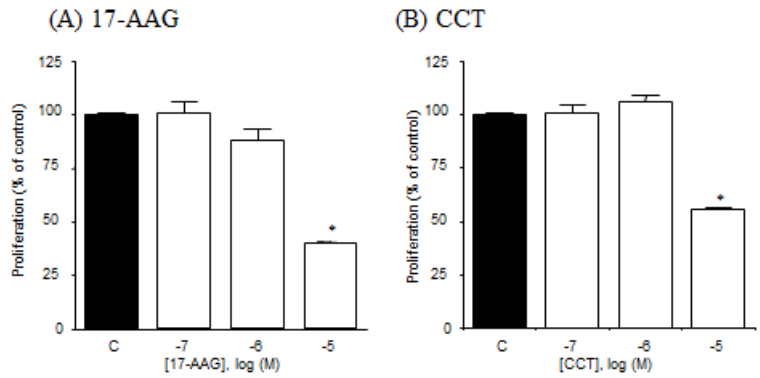

Fig.6.

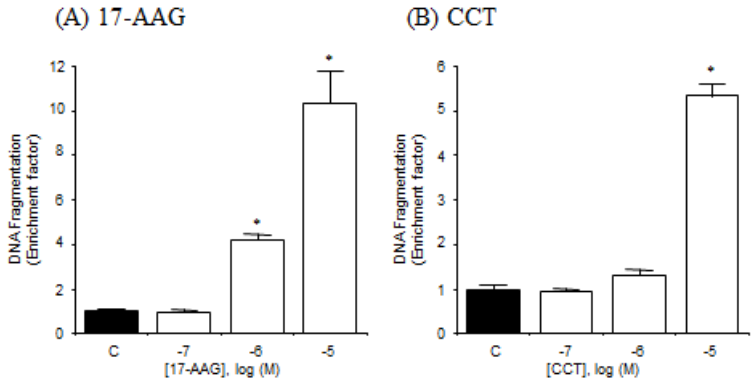

Fig.7.

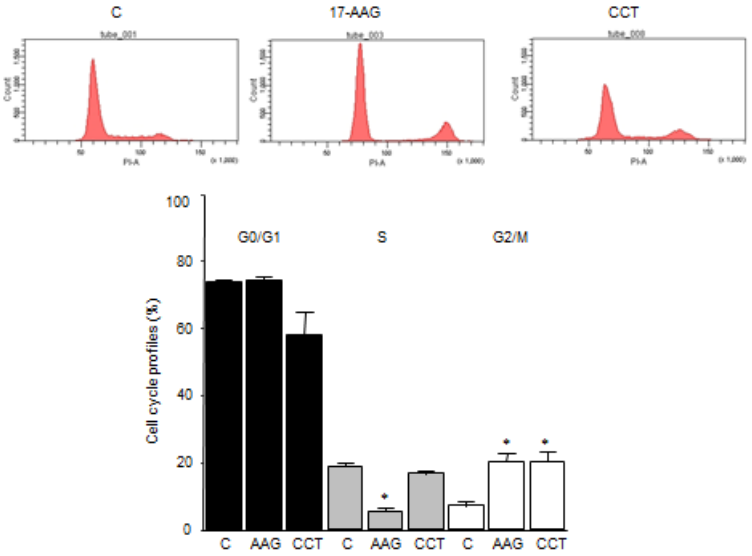

Fig.8.

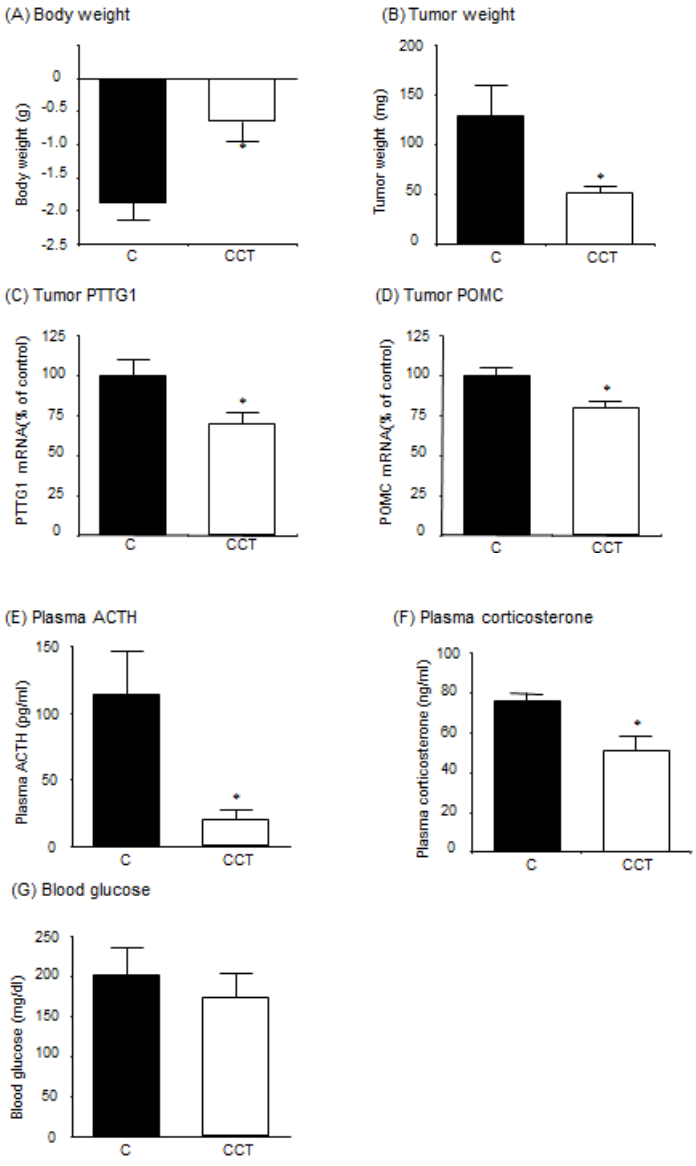
(A) Body weight
Body weight (g)
0
-0.5
-1.0
-1.5
-2.0
-2.5
C
CCT
(B) Tumor weight
Tumor weight (mg)
200
150
100
50
0
C
CCT
(C) Tumor PTTG1
PTTG1 mRNA(% of control)
125
100
75
50
25
0
C
CCT
(D) Tumor POMC
POMC mRNA(% of control)
125
100
75
50
25
0
C
CCT
(E) Plasma ACTH
Plasma ACTH (pg/ml)
150
100
50
0
C
CCT
(F) Plasma corticosterone
Plasma corticosterone (ng/ml)
100
80
60
40
20
0
C
CCT
(G) Blood glucose
Blood glucose (mg/dl)
250
200
150
100
50
0
C
CCT